Formability and magnetic properties of Dy-Co binary amorphous alloys

Cite as: AIP Advances **8**, 075215 (2018); https://doi.org/10.1063/1.5037357
Submitted: 23 April 2018 . Accepted: 05 July 2018 . Published Online: 17 July 2018

L. Y. Ma, B. Z. Tang, K. C. Chan, L. Zhao, M. B. Tang, D. Ding, and L. Xia

Formability and magnetic properties of Dy-Co binary amorphous alloys

L. Y. Ma,[1] B. Z. Tang,[1] K. C. Chan,[2,a] L. Zhao,[2] M. B. Tang,[3] D. Ding,[1] and L. Xia[1,2,a]

[1]*Laboratory for Microstructure, Institute of Materials, Shanghai University, Shanghai 200072, China*

[2]*Department of Industrial and Systems Engineering, The Hong Kong Polytechnic University, Hung Hom, Hong Kong*

[3]*Shanghai Institute of Ceramics, Chinese Academy of Science, Shanghai 200050, China*

(Received 23 April 2018; accepted 5 July 2018; published online 17 July 2018)

In this study, binary Dy-Co ribbons were synthesized by a conventional melt-spinning approach and glassy ribbons were successfully obtained within the compositional range $Dy_{50}Co_{50}$ to $Dy_{68}Co_{32}$. The glass formability and magnetic properties of these amorphous alloys were examined. The compositional dependence of glass formability, Curie temperature and magneto-caloric response of the Dy_xCo_{100-x} (x=50, 55, 60, 65 and 68) amorphous alloys, as well as the mechanism involved, were determined. https://doi.org/10.1063/1.5037357

I. INTRODUCTION

Amorphous alloys have huge scientific and industrial significance because of their superior properties resulting from their unique structure induced by fabrication conditions far from the equilibrium state.[1–4] Among these alloys, transition metal (TM) and rare earth (RE) based amorphous alloys have shown application potential because they exhibit pre-eminent magnetic properties. For instance, Nd(Pr)-TM-based bulk metallic glasses (BMGs) show anomalous large coercivity;[5,6] (Tb, Dy)-TM-based amorphous alloys exhibit extraordinary magnetostriction;[7–9] and Gd-Co-based metallic glasses exhibit an outstanding magnetocaloric effect (MCE).[10–18]

Gd-TM-based glassy alloys possess a second order magnetic phase transition (MPT), which leads to a broadened magnetic entropy change ($-\Delta S_m$) peak and also an ultra-high refrigeration capacity. However, the peak of $-\Delta S_m$ ($-\Delta S_m{}^{peak}$) of the Gd-TM-based glassy alloys is usually inferior to that of the intermetallic compounds undergoing a first order MPT. Therefore, it is essential to find ways to enhance the value of the $-\Delta S_m{}^{peak}$ of Gd-TM-based amorphous alloys.

One of the valid methods to improve the MCE and formability of Gd-TM-based amorphous alloys is to replace the Gd elements by other RE metals, such as Tb, Dy, Ho, Er, Y and so on.[16–18] However, the addition of Tb and Dy may induce spin-glass-like behavior and make the magnetic entropy change of the amorphous alloys irreversible.[18,19] Therefore, systematic investigation of the formability and magnetic properties of Tb/Dy-TM binary amorphous alloys can be a simple but valid way to understand the influence of the addition of Tb or Dy on the formability and MCE of amorphous alloys in more detail.

In this investigation, we studied the glass formability and magnetic properties of a representative binary Dy-Co amorphous alloy system. The amorphous Dy-Co alloys were prepared as ribbons by the conventional melt-spinning method, and the best composition for glass formation in this alloy system was identified. The compositional dependence of the glass formability, Curie temperature (T_c) and $-\Delta S_m$ of the binary glassy alloys were constructed, and the mechanisms were investigated.

[a]Corresponding authors. Email: kc.chan@polyu.edu.hk (K. C. Chan) & xialei@shu.edu.cn (L. Xia)

The findings are helpful for understanding the formability, T_c and magnetocaloric responses of Tb/Dy-TM-based amorphous alloys.

II. EXPERIMENTAL PROCEDURES

Dy_xCo_{100-x} (x=45, 50, 55, 60, 65, 68, 70 and 75) alloys were fabricated by arc-melting mixtures of high purity Dy (99.9 at. %) and Co (99.9 at. %) metals under a Ti-gettered argon atmosphere. Binary Dy_xCo_{100-x} ribbons were fabricated by spinning the melting liquid on a copper wheel with a surface linear velocity of 30 m/s under a highly purified argon atmosphere. The approximate width of the as-prepared ribbon was 1 mm and the average thickness was about 40 μm. The structure state of the Dy_xCo_{100-x} ribbons was confirmed using X-ray diffraction (XRD) analysis with Cu K_α radiation (Rigaku D\max-2550). High resolution electron microscopy (HREM) observations were performed using a JEOL JEM-2010F high resolution electron microscope to ascertain the disordered microstructure of the amorphous ribbons. Specimens for HREM observation were prepared by ion-polishing under a pure argon atmosphere using the GATAN 691 precision ion-polishing system. The thermal properties of the Dy_xCo_{100-x} amorphous ribbons were measured using differential scanning calorimetry (DSC, Perkin-Elmer DIAMOND) under a highly purified argon atmosphere at a constant heating rate of 20 K/min. The magnetic properties of the Dy_xCo_{100-x} ribbons were acquired using a Quantum Design Physical Properties Measurement System (PPMS 6000). The temperature dependence of the magnetization (M-T) curves were obtained under a magnetic field of 0.03 T in the heating process after cooling from room temperature to 10 K under a zero field (ZFC) or a magnetic field of 0.03 T (FC). The hysteresis loops and the isothermal magnetization (M-H) curves were obtained at different selected temperatures under a magnetic field of 5 T.

III. RESULTS AND DISCUSSION

Figure 1 displays the XRD patterns of the obtained Dy_xCo_{100-x} (x=45, 50, 55, 60, 65, 68, 70 and 75) ribbons. The broadened diffraction maxima in the XRD patterns of the as-spun $Dy_{50}Co_{50}$, $Dy_{55}Co_{45}$, $Dy_{60}Co_{40}$, $Dy_{65}Co_{35}$ and $Dy_{68}Co_{32}$ ribbons reveal the typical amorphous features of these samples. In contrast, the $Dy_{45}Co_{55}$, $Dy_{70}Co_{30}$ and $Dy_{75}Co_{25}$ are partially or fully crystallized.

A. Glass forming ability of the Dy-Co binary alloys

The DSC curves for the Dy_xCo_{100-x} (x=50, 55, 60, 65 and 68) amorphous ribbons are shown in Fig. 2(a). The amorphous characteristics of these ribbons are further verified by the typical endothermic glass transition and exothermic crystallization behavior in the DSC curves. The onset temperature for glass transition (T_g) and crystallization (T_x) of each amorphous ribbon, as marked clearly in Fig. 2(a), are listed in Table I. Therefore, associated with the liquidus temperatures (T_l) of the alloys acquired from the binary phase diagram,[20] we calculated the reduced glass transition temperature

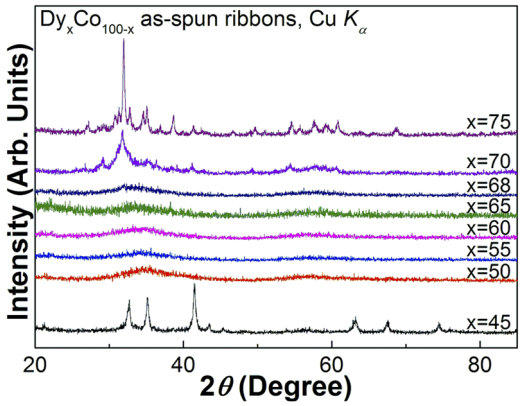

FIG. 1. XRD patterns of the Dy_xCo_{100-x} (x=45, 50, 55, 60, 65, 68, 70, 75) as-spun ribbons prepared at the surface linear velocity of 30 m/s.

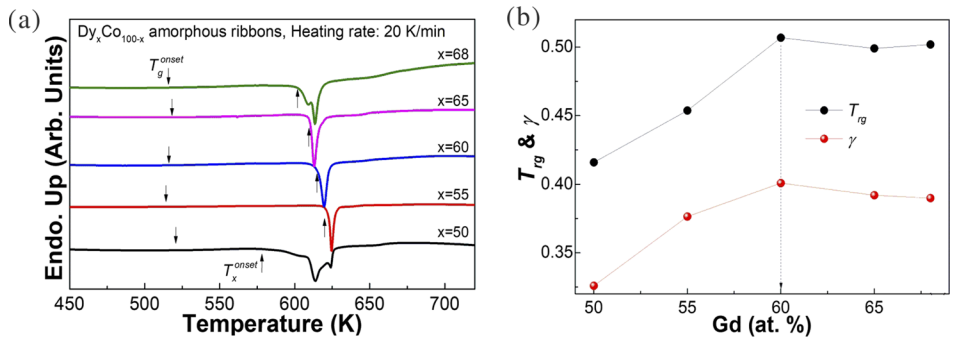

FIG. 2. **(a)** The continuous DSC curves of the Dy_xCo_{100-x} (x=50, 55, 60, 65 and 68) ribbons obtained at a constant heating rate of 20 K/min, and **(b)** the compositional dependence of T_{rg} and γ of the Dy_xCo_{100-x} amorphous ribbons.

(T_{rg})[3] and the parameter γ (=T_x/(T_g+T_l))[21] of the Dy_xCo_{100-x} (x=50, 55, 60, 65 and 68) amorphous alloys. This enabled investigation of the formability of the amorphous alloys because the above two parameters are the most widely used gauges for evaluating the formability of metallic glasses. The compositional dependence of T_{rg} and γ of the Dy_xCo_{100-x} amorphous ribbons is shown in Fig. 2(b). It is clear that the eutectic $Dy_{60}Co_{40}$ provides the best composition for glass forming in the Dy-Co alloy system, which is in accord with the deep eutectic rule for predicting the glass formability of the alloys.[21,22]

B. Magnetic properties of the amorphous alloys

Figure 3(a) displays the ZFC and FC *M-T* curves of the $Dy_{55}Co_{45}$ amorphous ribbon. The ZFC *M-T* curve nearly overlaps with the FC *M-T* curve within the temperature range 70 - 300 K and diverges from the FC *M-T* curve at temperatures lower than 70 K. The difference between the ZFC and FC *M-T* curves of the $Dy_{55}Co_{45}$ amorphous ribbon is analogous to those of spin glass systems.[8,18,19] The spin-glass-like behavior is also illustrated by the *M-H* curves of the $Dy_{55}Co_{45}$ amorphous ribbon, as demonstrated in the upper-right inset of Fig. 3(a). The decreasing magnetization under a very low magnetic field from 50K to 10 K indicates the typical spin glass behavior of the $Dy_{55}Co_{45}$ amorphous ribbon. However, this kind of ZFC-FC curve and M-H curve can also be found in nano-structured amorphous composites as a result of their superparamagnetic behavior. Therefore, HREM observation of the $Dy_{55}Co_{45}$ ribbon was undertaken to ascertain the disordered microstructure of the as-spun ribbons. Figure 4 shows the HREM image of the as-spun ribbon. The $Dy_{55}Co_{45}$ as-spun ribbon is fully amorphous with only short ranged orders, and no obvious crystalline phases or small grains have been found in the amorphous matrix.

TABLE I. Thermal and magnetic properties of the Dy_xCo_{100-x} amorphous ribbons.

Dy_xCo_{100-x} ribbons	T_g^{onse} (K)	T_x^{onset} (K)	T_l (K)	T_{rg}	γ	T_c (K)	T_f (K)
x=50	521	578	1253	0.416	0.326	106	80
x=55	514	620	1133	0.454	0.376	73	55
x=60	516	615	1018	0.507	0.401	54	45
x=65	518	610	1038	0.499	0.392	46	35
x=68	516	602	1028	0.502	0.390	43	33

Dy_xCo_{100-x} ribbons	$-\Delta S_m^{peak}$ (J K-1 kg-1)				
	1 T	1.5 T	2 T	3 T	5 T
x=50	1.8	2.55	3.24	4.53	6.82
x=55	2.5	3.5	4.41	6.05	8.75
x=60	3.19	4.43	5.53	7.41	10.39
x=65	3.65	5	6.19	8.2	11.3
x=68	3.81	5.3	6.59	8.86	12.58

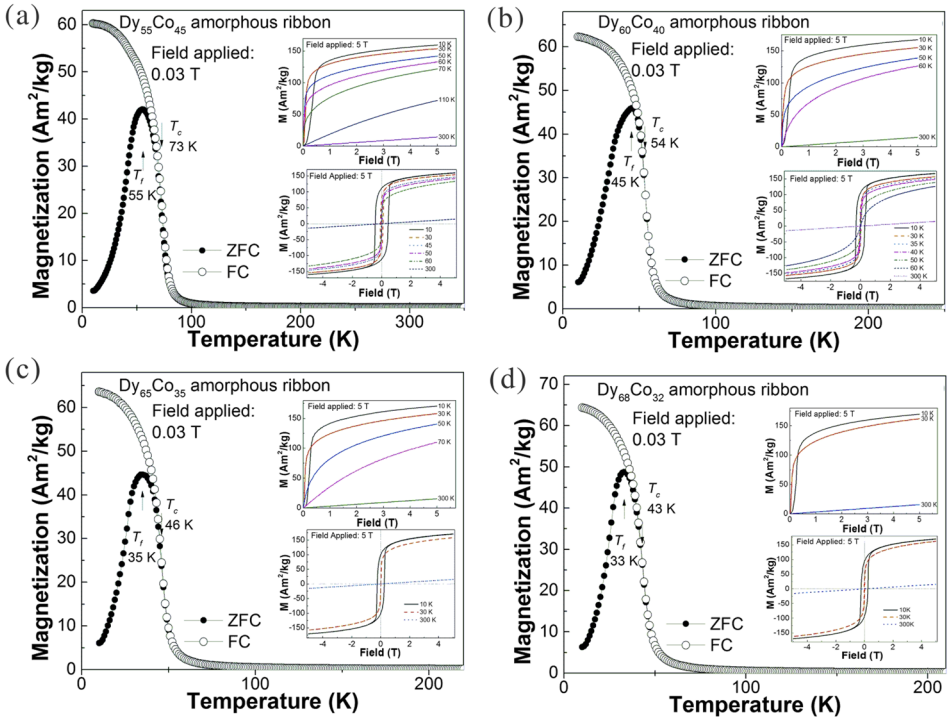

FIG. 3. ZFC and FC *M-T* curves, Curie temperatures (T_c) and spin freezing temperatures (T_f), *M-H* curves (upper right inset) and hysteresis loops (lower right inset) of the **(a)** $Dy_{55}Co_{45}$, **(b)** $Dy_{60}Co_{40}$, **(c)** $Dy_{65}Co_{35}$ and **(d)** $Dy_{68}Co_{32}$ ribbons.

It is known that Dy(Tb)-based amorphous systems involve huge random magnetic anisotropy (RAM) due to the local random electrostatic field. According to the random anisotropy model, the RMA existing in amorphous alloys will break the rotational symmetry of the Hamiltonian and increase the hysteresis.[8,23] The hysteresis loops of the $Dy_{55}Co_{45}$ amorphous ribbon were measured under a magnetic field of 5 T at 10 K, 30 K, 45 K, 50 K, 60 K and 300 K, respectively, as displayed in the lower-right inset of Fig. 3(a). The ribbon is paramagnetic at ambient temperatures and is soft magnetic with nearly zero coercivity from 50 K to 60 K, but is hard magnetic at 10 K and 45 K. The coercivity is about 0.03 T at 45 K, about 0.09 T at 30 K and about 0.46 T at 10 K, all due to the strong RMA at lower temperatures. The decreased coercivity with increasing temperature is due to the unfreezing of the magnetic moment due to the thermal fluctuation. T_c of the $Dy_{55}Co_{45}$ amorphous ribbon is about 73 K, and the spin freezing temperature (T_f) is about 55 K.

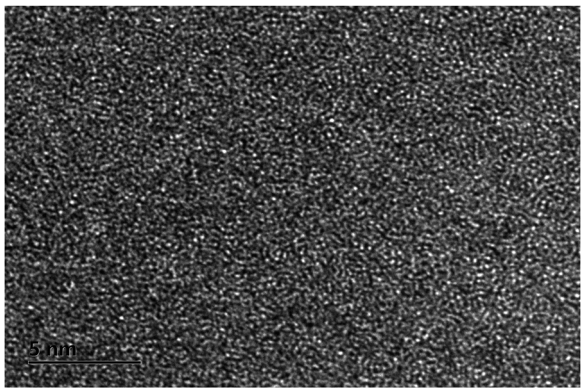

FIG. 4. HREM image of the $Dy_{55}Co_{45}$ as-spun ribbon.

The *M-T* (including ZFC and FC) curves, *M-H* curves and hysteresis loops of the other Dy_xCo_{100-x} amorphous ribbons are shown in Fig. 3(b) for x=60, Fig. 3(c) for x=65 and Fig. 3(d) for x=68. Agreeing with our preliminary work on $Dy_{50}Co_{50}$ amorphous ribbons,[24] all the Dy_xCo_{100-x} amorphous ribbons show spin-glass-like behavior. The Curie temperatures and spin freezing temperatures for the Dy_xCo_{100-x} (x=50, 55, 60, 65 and 68) amorphous ribbons are also listed in Table I.

One of the characteristics of amorphous alloys that is superior to intermetallic compounds is that T_c of the amorphous alloys can be adjusted by customizing the composition of the alloys. In our previous work, we found a linear relationship between the Gd content and T_c in Gd-Co binary amorphous alloys. The compositional dependence of T_c of RE-Co-based amorphous alloys was investigated. Based on the model of Rudermann-Kittel-Kasuya-Yosida indirect interaction,[16] a linear relationship between T_c and the de Gennes factor (G) was found in various RE-Co-based amorphous alloys. For amorphous alloys containing only one RE element, the G factor is proportional to the molar fraction of the RE atoms. Therefore, from the viewpoint of 4*f*-4*f* indirect interaction, the compositional dependence of T_c in Dy-Co amorphous alloys should be linear. However, in addition to the 4*f*-4*f* indirect interaction between the RE-RE atoms, there are two other kinds of interactions in RE-TM-based amorphous alloys: 3*d*-3*d* direct interaction between the TM-TM atoms and the 3*d*-4*f* indirect interaction between the RE-TM atoms. The influence of 3*d*-3*d* direct interaction on the Curie temperature in the RE-TM-based amorphous alloys is supposed to be similar to that of the 4*f*-4*f* indirect interaction. This is understandable because there is only (100%) 3*d*-3*d* direct interaction in a pure TM metal and no (0%) 3*d*-3*d* direct interaction in alloys free of TM elements. The contribution of the 3*d*-3*d* direct interaction is proportional to the molar fraction of the Co element in Dy-Co amorphous alloys and the compositional dependence of T_c in Dy-Co amorphous alloys is still linear from the viewpoint of 3*d*-3*d* direct interaction. However, the effect of 3*d*-4*f* indirect interaction on the Curie temperature in RE-TM-based amorphous alloys is more complicated. The 3*d*-4*f* indirect interaction exists in RE-TM amorphous alloys but does not exist in either RE free or TM free alloys, which means that the compositional dependence of the 3*d*-4*f* indirect interaction in Dy-Co amorphous alloys will not be linear. As a result, the compositional dependence of T_c, determined by the three kinds of interactions in RE-TM-based amorphous alloys, is not linear. Figure 5 displays the compositional dependence of T_c for the Dy_xCo_{100-x} glassy ribbons. The non-linear T_c-Dy (at. %) curve indicates that the non-linear compositional dependence of the 3*d*-4*f* indirect interaction plays a significant role in dominating the Curie temperature of Dy-Co amorphous alloys. The nearly linear dependence of T_c on the Gd content in Gd-Co amorphous alloys[25] is likely due to the negligible 3*d*-4*f* indirect interaction compared to the 3*d*-3*d* direct interaction and 4*f*-4*f* indirect interaction in Gd-Co binary amorphous alloys.

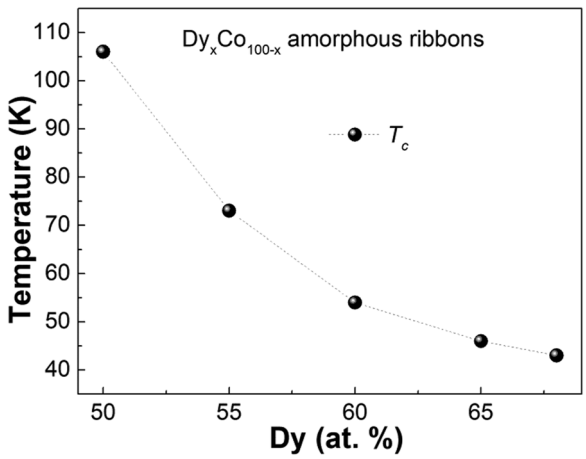

FIG. 5. The compositional dependence of T_c for the Dy_xCo_{100-x} (x=50, 55, 60, 65 and 68) ribbons.

C. Magneto-caloric response of the amorphous alloys

The spin freezing behavior is reported to make the magnetic entropy change irreversible at temperatures well below T_f and reduce the magneto-caloric properties of Dy-based bulk metallic glasses.[18,19] Therefore, we determined the temperature dependence of $-\Delta S_m$ from the *M-H* curves of the Dy_xCo_{100-x} amorphous ribbons above T_f, as shown in Fig. 6. The $-\Delta S_m{}^{peak}$ of the Dy_xCo_{100-x} amorphous ribbons clearly increases with the decreasing Dy concentration. However, the MCE of the Dy-Co amorphous alloys is not so significant when compared to that of the Gd-Co-based amorphous alloys. This is possibly because that Gd has no orbital momentum with a relatively low magneto-crystalline anisotropy.[10–18,28]

The dependence of $-\Delta S_m{}^{peak}$ on the T_c of the amorphous alloys is usually described by the $-\Delta S_m{}^{peak} \propto T_c{}^{-2/3}$ relationship, as proposed by Belo *et al.*, according to the mean field theory approach.[26] According to the $-\Delta S_m{}^{peak}$ values for the Dy_xCo_{100-x} amorphous ribbons under the various magnetic fields listed in Table I, we constructed $\ln(-\Delta S_m{}^{peak})$ *vs* $\ln(T_c)$ plots under various fields for the amorphous alloys, as shown in Fig. 7(a). By linear fitting of the $\ln(-\Delta S_m{}^{peak})$ vs $\ln(T_c)$ plots, we obtained the $-\Delta S_m{}^{peak} \propto T_c{}^{m}$ relationship for amorphous alloys: where m= −0.85 under 1 T; m= −0.82 under 1.5 T; m= −0.8 under 2 T; m= −0.74 under 3 T and m= −0.66 under 5 T. Although the m value approximates to −2/3 under a field of 5 T, it is much lower than −2/3 under magnetic fields lower than 5 T, indicating that the $-\Delta S_m{}^{peak}$-T_c relationship of Dy_xCo_{100-x} amorphous alloys is different from the mean field theory prediction.

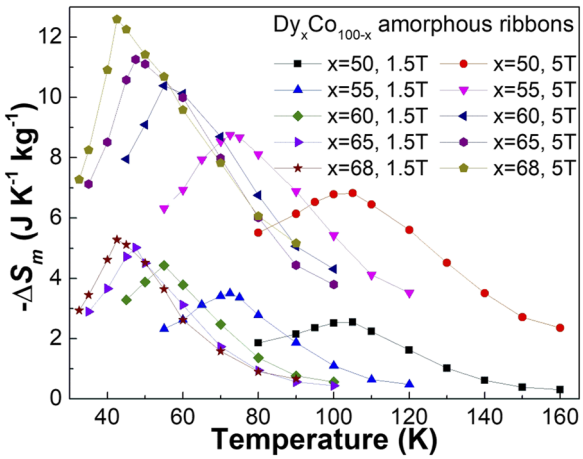

FIG. 6. The $(-\Delta S_m)$-T curves of the Dy_xCo_{100-x} (x=50, 55, 60, 65 and 68) ribbons under the magnetic fields of 1.5 T and 5 T.

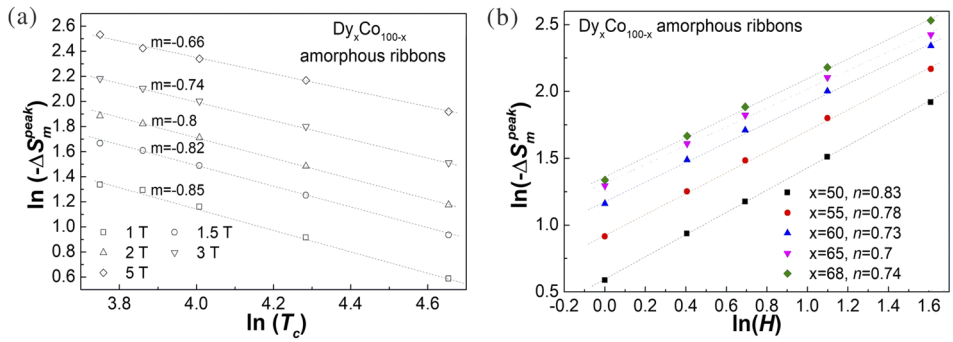

FIG. 7. **(a)** The linear fittings of the $\ln(T_c)$ *vs* $\ln(-\Delta S_m{}^{peak})$ plots under various fields, and **(b)** the linear fittings of $\ln(H)$ *vs* $\ln(-\Delta S_m{}^{peak})$ plots for the Dy_xCo_{100-x} (x=50, 55, 60, 65 and 68) ribbons.

The deviation of the $-\Delta S_m{}^{peak}$-T_c relationship of the Dy_xCo_{100-x} amorphous alloys from the mean field prediction can also be verified by the $-\Delta S_m \propto H^n$ relationship of each amorphous ribbon. Figure 7(b) shows the linear fitting of $\ln(H)$ *vs* $\ln(-\Delta S_m{}^{peak})$ for the Dy_xCo_{100-x} amorphous alloys. The n value near T_c is about 0.83 for x=50, 0.78 for x=55, 0.73 for x=60, 0.7 for x=65 and 0.74 for x=68, all of which are larger than the value predicted from the mean field theory, but agree well with the results predicted by the Arrott-Noakes equation, according to the typical microstructure of amorphous alloys with numerous short range orders embedded in the disordered matrix.[12,27]

IV. CONCLUSIONS

In summary, the glass formability and magnetic properties of the binary Dy-Co amorphous alloys were investigated in this work. Dy-Co ribbons were fabricated by the melt-spinning method at a wheel surface velocity of 30 m/s and Dy_xCo_{100-x} (x=50, 55, 60, 65 and 68) amorphous ribbons were obtained. The glass formability of the Dy-Co binary alloys was examined, and the best composition for glass formation was found to be the $Dy_{60}Co_{40}$ alloy, which agrees well with the deep eutectic rule. The magnetic properties and the magnetocaloric response for the amorphous alloys were also investigated. It was found that the Curie temperature decreases with the augmenting Dy concentration. The compositional dependence of T_c shows a non-linear relationship, indicating that the non-linear compositional dependence of the $3d$-$4f$ indirect interaction plays a vital role in dominating the Curie temperature of Dy-Co binary amorphous alloys. All the Dy_xCo_{100-x} amorphous ribbons show spin-glass-like behavior, with the spin freezing temperatures obtained. The $(-\Delta S_m)$-T curves of the Dy_xCo_{100-x} amorphous ribbons were constructed at temperatures above T_f to avoid the irreversible magnetic entropy change induced by the spin-glass-like behavior of the amorphous alloys. The dependence of $-\Delta S_m{}^{peak}$ on the Curie temperature, as well as the magnetic field, was investigated. The deviation of the magneto-caloric behavior of the Dy_xCo_{100-x} amorphous alloys from the mean field prediction was ascertained by both the $(-\Delta S_m{}^{peak})$-T_c and the H-$(-\Delta S_m{}^{peak})$ relationships.

ACKNOWLEDGMENTS

The work described in this paper was supported by the National Nature Science Foundation of China (Grant Nos. 51271103 and 51671119), and by a grant from the Research Grants Council of the Hong Kong Special Administrative Region, China (Project No. PolyU 15253916).

[1] M. Miller and P. Liaw, *Bulk Metallic Glasses* (Springer, 2008).
[2] C. Suryanarayana and A. Inoue, *Bulk metallic glasses* (CRC Press, 2011).
[3] D. Turnbull, "Under what conditions can a glass be formed?," Contemp. Phys. **10**, 473–488 (1969).
[4] W. L. Johnson, J. H. Na, and M. D. Demetriou, "Quantifying the origin of metallic glass formation," Nat. Commun. **7**, 11516 (2016).
[5] A. Inoue, T. Zhang, W. Zhang, and A. Takeuchi, "Bulk Nd-Fe-Al amorphous alloys with hard magnetic properties," Mater. Trans. JIM **37**, 99–108 (1996).
[6] L. Xia, S. S. Fang, C. L. Jo, and Y. D. Dong, "Glass forming ability and microstructure of hard magnetic $Nd_{60}Al_{20}Fe_{20}$ glass forming alloy," Intermetallics **14**, 10981101 (2006).
[7] A. Speliotis and D. Niarchos, "Magnetostrictive properties of amorphous and crystalline TbDyFe thin films," Sens. Actuators A **106**, 298 (2003).
[8] T. Speliotis and D. Niarchos, "Extraordinary magnetization of amorphous TbDyFe films," Microelectro. Eng. **112**, 183 (2013).
[9] B. Z. Tang, D. Q. Guo, L. Xia, D. Ding, and K. C. Chan, "Magnetoelastic and magnetocaloric properties of $Tb_{62.5}Co_{37.5}$ amorphous alloy," J. Alloys Compd. **728**, 747–751 (2017).
[10] Z. W. Wang, P. Yu, Y. T. Cui, and L. Xia, "Near room temperature magneto-caloric effect of a $Gd_{48}Co_{52}$ amorphous alloy," J. Alloys Compd. **658**, 598–602 (2016).
[11] Q. Luo, M. B. Tang, and J. Shen, "Tuning the magnetocaloric response of Er-based metallic glasses by varying structural order in disorder," J. Magn. Magn. Mater. **401**, 406–411 (2016).
[12] L. Xia, Q. Guan, D. Ding, M. B. Tang, and Y. D. Dong, "Magneto-caloric response of the $Gd_{60}Co_{25}Al_{15}$ metallic glasses," Appl. Phys. Lett. **105**, 192402 (2014).
[13] X. C. Zhong, X. W. Huang, X. Y. Shen, H. Y. Mo, and Z. W. Liu, "Thermal stability, magnetic properties and large refrigerant capacity of ternary $Gd_{55}Co_{35}M_{10}$ (M=Mn, Fe and Ni) amorphous alloys," J. Alloys Compd. **682**, 476–480 (2016).
[14] G. L. Liu, D. Q. Zhao, H. Y. Bai, W. H. Wang, and M. X. Pan, "Room temperature table-like magnetocaloric effect in amorphous $Gd_{50}Co_{45}Fe_5$ ribbon," J. Phys. D: Appl. Phys. **49**, 055004 (2016).
[15] L. Y. Ma, L. H. Gan, K. C. Chan, D. Ding, and L. Xia, "Achieving a table-like magnetic entropy change across the ice point of water with tailorable temperature range in Gd-Co-based amorphous hybrids," J. Alloys Compd. **723**, 197–200 (2017).

[16] H. Zhang, R. Li, L. Zhang, and T. Zhang, "Tunable magnetic and magnetocaloric properties in heavy rare-earth based metallic glasses through the substitution of similar elements," J. Appl. Phys. **115**, 133903 (2014).
[17] Y. Liu, J. Zhang, Y. Wang, Y. Zhu, Z. Yang, J. Chen, and S. Cao, "Weak exchange effect and large refrigerant capacity in a bulk metallic glass $Gd_{0.32}Tb_{0.26}Co_{0.20}Al_{0.22}$," Appl. Phys. Lett. **94**, 112507 (2009).
[18] Q. Luo, P. N. Dinh, X. Kou, and J. Shen, "Controllable ferromagnetic/re-entrant spin glass state and magnetocaloric response of Gd-Er-Al-Co metallic glasses," J. Alloys Compd. **725**, 835–839 (2017).
[19] Q. Luo, B. Schwarz, N. Mattern, and J. Eckert, "Irreversible and reversible magnetic entropy change in a Dy-based bulk metallic glass," Intermetallics **30**, 76–79 (2012).
[20] T. B. Massalski, H. Okamoto, P. R. Subramanian, and L. Kacprzak, *Binary Alloy Phase Diagrams*, 2nd ed. (ASM international, 1990).
[21] Z. P. Lu and C. T. Liu, "Glass formation criterion for various glass-forming systems," Phys. Rev. Lett. **91**, 115505 (2003).
[22] A. Inoue, "Stabilization of metallic supercooled liquid and bulk amorphous alloys," Acta Mater. **48**, 279–306 (2000).
[23] R. Harris, M. Plischke, and M. J. Zuckermann, "New model for amorphous magnetism," Phys. Rev. Lett. **31**, 160 (1974).
[24] L. Xia, K. C. Chan, D. Ding, L. Zhao, and B. Z. Tang, "Magnetic properties and magnetostriction of a binary $Dy_{50}Co_{50}$ amorphous alloy," J. Non-Cryst. Solids **493**, 29–32 (2018).
[25] C. Wu, D. Ding, L. Xia, and K. C. Chan, "Achieving tailorable magneto-caloric effect in the Gd-Co binary amorphous alloys," AIP Adv. **6**, 035302 (2016).
[26] J. H. Belo, J. S. Amaral, A. M. Pereira, V. S. Amaral, and J. P. Araújo, "On the Curie temperature dependency of the magnetocaloric effect," Appl. Phys. Lett. **100**, 242407 (2012).
[27] V. Franco, J. M. Borrego, C. F. Conde, A. Conde, M. Stoica, and S. Roth, "Refrigerant capacity of FeCrMoCuGaPCB amorphous alloys," J. Appl. Phys. **100**, 083903 (2006).
[28] J. Du, Q. Zheng, Y. B. Li, Q. Zhang, D. Li, and Z. D. Zhang, "Large magnetocaloric effect and enhanced magnetic refrigeration in ternary Gd-based bulk metallic glasses," J. Appl. Phys. **103**, 023918 (2008).